Neutron Scattering from Pressurized Polyolefin Blends near the Limits of Metastability

Amy A. Lefebvre, Joon H. Lee, and Nitash P. Balsara*,†

Department of Chemical Engineering, Chemistry and Materials Science, Polytechnic University, Six Metrotech Center, Brooklyn, New York 11201

Boualem Hammouda

National Institute of Standards and Technology, Building 235, E 151, Gaithersburg, Maryland 20899

Received March 14, 2000; Revised Manuscript Received July 18, 2000

ABSTRACT: Small-angle neutron scattering experiments were conducted on a series of off-critical binary polymethylbutylene/polyethylbutylene (PMB/PEB) blends over a wide range of blend compositions, component molecular masses, temperatures, and pressures. The blends become more immiscible with either decreasing temperature or increasing pressure. A simple extension of the Flory−Huggins theory that accounts for finite volume changes of mixing (ΔV) is presented. Our extension demonstrates the validity of the usual mean-field theory of scattering from polymer mixtures based on the random phase approximation (RPA) at elevated pressures. We use this framework to analyze the temperature and pressure dependence of the small-angle neutron scattering profiles obtained from binary PMB/PEB blends. We propose that the volume change of mixing is a linear response to the repulsive interactions between monomers. We demonstrate that off-critical PMB/PEB blends can be undercooled or superpressurized deep into the metastable two-phase region (e.g., up to 50 °C undercooling) without detectable signs of phase separation. The χ parameters and the statistical segment lengths obtained by fitting the data obtained in the metastable region are within experimental error of those determined from stable, single-phase PMB/PEB blends well-removed from a phase boundary. This indicates that the concentration fluctuations in the metastable region of the phase diagram have a mean-field character similar to those in stable, single-phase blends that have been extensively characterized by the RPA-based theory.

Introduction

There is continuing interest in the effect of pressure on the thermodynamics of polymer blends and block copolymers.[1−15] Typical experimental results that have been obtained are shown in Figure 1, where we show a schematic phase diagram for a binary polymer blend in temperature−composition ($T-\phi_1$) space (ϕ_1 is the volume fraction of one of the components). It has been found that changing the system pressure, say from P_1 to P_2, results in a shift of the phase boundary as shown in Figure 1. Two kinds of experiments have been used to demonstrate this. In the first type of experiment, a system in the homogeneous part of the phase diagram (e.g., point I in Figure 1) is studied as a function of pressure at constant temperature and composition. As the phase boundary approaches point I with changing pressure, the concentration fluctuations increase in magnitude. This can be detected using either small-angle neutron scattering (SANS) or small-angle X-ray scattering (SAXS). We refer to this kind of experiment as a type I experiment. In the second kind of experiment, the location of the phase boundary of a particular system is studied as a function of pressure. The dependence of the cloud point of a blend can be detected by light scattering under pressure. On the other hand, the order−disorder transition temperature of a block copolymer can be detected by depolarized light scattering under pressure.[15] Such experiments yield information about the dependence of the phase transition temperature (T_p) on P. We refer to this kind of experiment as a type II experiment.[1,3,5,9,12,14,15]

The interpretation of scattering data from polymer mixtures was facilitated by the pioneering work of de Gennes, who developed the random phase approximation (RPA).[16] The original derivation was restricted to binary polymer blends, and it was based on the postulate that concentration fluctuations are driven by mean-field potentials. The local concentrations of the two components were assumed to be coupled due to the incompressibility of the mixture [$\phi_1(\mathbf{r}) + \phi_2(\mathbf{r}) = 1$ at all locations $\mathbf{r}$ in the blend], and this led to a self-consistent analysis for determining the potentials. The final result was a simple expression for the scattering intensity from single-phase polymer blends in terms of the statistical segment lengths of the polymer chains (scaling of chain radius of gyration with molecular mass) and the Flory−Huggins interaction parameter χ, which, in theory, is related to the energy of interaction between monomers. All other nonidealities of mixing, including

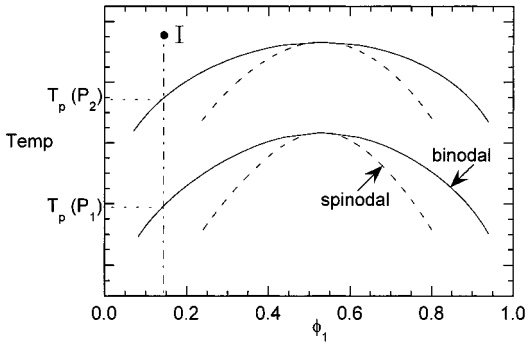

Figure 1. A schematic phase diagram for polymer blends at pressures P_1 and P_2 in T versus ϕ_1 format, where T is temperature and ϕ_1 is the volume fraction of component 1. The solid curve is the binodal curve, and the dashed curve is the spinodal curve. In a type I experiment, a single-phase blend (e.g., point I) is studied as a function of pressure. In a type II experiment the phase transition temperature (T_p) is studied as a function of pressure.

† Permanent address: Department of Chemical Engineering, University of California, Berkeley, CA 94720.

10.1021/ma000462x CCC: $19.00
Published on Web 09/23/2000

volume changes of mixing (ΔV), were assumed to be negligible. Subsequent work by Leibler and others enables the application of the RPA-based framework to any multicomponent polymer mixture, regardless of the number of components and their architectural complexity.[17−20]

Some researchers have used the RPA-based equations to analyze pressure-dependent scattering data from type I experiments on blends and block copolymers. In all cases,[1,3,4,6−8,10,11] the data from homogeneous, one-phase systems are consistent with the RPA if χ and the statistical segment lengths are assumed to be pressure dependent. This is in addition to the usual temperature dependence of these parameters.[21−23] Other groups have questioned the applicability of the RPA to type I experiments because of the incompressibility assumption, and different modifications of the original RPA have been proposed.[1,4,8]

The data obtained in type II experiments are invariably analyzed by using the Clausius−Clayperon equation,[24]

$$dT_p/dP = T\Delta V_p/\Delta H_p \qquad (1)$$

where ΔV_p and ΔH_p are the volume and enthalpy changes associated with the phase transition.

Janssen et al.[1] obtained χ in deuterated polystyrene/poly(vinyl methyl ether) (dPS/PVME) blends by the application of the RPA to SANS data. They also estimated χ from *PVT* measurements on the pure components and the blends, using the Flory−Orwoll−Vrij equation of state. The χ parameters, determined from the two techniques, were in reasonable agreement. Hammouda et al. studied the pressure dependence of χ in dPS/poly(butyl methacrylate) (dPS/PBMA) and dPS/PVME blends.[7,8] In ref 8 they implemented a scheme for analyzing the SANS data, using a model that combines a compressible RPA model with one that accounts for the presence of free volume.[25] In this approach, the interpolymer interactions are not described by a χ parameter. Hajduk et al. studied the pressure dependence of χ in disordered polystyrene-*block*-polyisoprene (PS−PI) copolymer melts.[4] They used a modified RPA-based approach proposed by Tang and Freed[26] to estimate χ as a function of T and P. Using the idea that χN (where N is the number of monomers per chain) at the order−disorder transition must be a constant, they estimated that dT_p/dP to be 10 °C/kbar for their system. Explicit measurements of dT_p/dP by Hajduk et al.[5] indicated that $dT_p/dP = 20$ °C/kbar. To our knowledge, this work represents the first attempt to reconcile the results of type I and type II experiments in polymeric mixtures. Rabeony et al.[6] studied a variety of polyolefin blends. They found that the temperature and pressure dependence of the χ parameter for different systems collapsed onto a master curve when χ was plotted as a function of density. The density of the mixtures were computed from the known densities of the pure components, assuming $\Delta V = 0$. They thus proposed that the pressure dependence of χ is due to the pressure dependence of the interaction energy between the monomers.

It is clear that despite considerable previous efforts,[1,4−8] several questions about the interpretation of pressure-dependent scattering from polymer mixtures remain unresolved:

(1) Experimentalists seldom question the applicability of the RPA at atmospheric pressure. Why then have some experimentalists not used the RPA to analyze data obtained at elevated pressures? Does the applicability of the RPA decrease with increasing pressure?

(2) What is the microscopic origin of the pressure dependence of the measured χ parameter?

(3) How can one reconcile the results of the RPA-based analysis of type I experiments wherein ΔV is assumed to be zero and the results of the Clausius−Clayperon analysis of type II experiments which requires ΔV to be finite for a measurable pressure effect?

(4) Is eq 1, the one-component Clausius−Clayperon equation, a good approximation for phase transitions in polymer blends and block copolymers?

Our objective is to provide answers to these questions. We propose a simple extension of the Flory−Huggins theory that accounts for finite ΔV and demonstrates the validity of the RPA at elevated pressures. An important conclusion is that the pressure dependence of SANS (or SAXS) data in type I experiments must arise from finite ΔV. We conducted experiments to explore the validity of our approach and the limits of applicability of the RPA. A series of binary polymethylbutylene/polyethylbutylene (PMB/PEB) blends were studied by SANS over a wide range of blend compositions, component molecular masses, temperatures, and pressures.

In addition to answering the questions raised in the previous paragraphs, we also consider whether RPA can be applied to metastable systems. It is clear that the RPA applies to stable, one-phase systems, i.e., systems located outside the binodal curve at a given T and P (see Figure 1). It is also clear that the RPA is not applicable to unstable systems located within the spinodal curve at a given T and P (see Figure 1). In the case of unstable systems, the blend structure is time-dependent, and the scattering intensity profiles computed using the RPA contain an unphysical singularity (a pole) at finite scattering vector q. However in the metastable region, i.e., in the region between the binodal and spinodal curves (see Figure 1), nucleation barriers can stabilize single-phase systems for some time, and there are no singularities in the RPA-based scattering profiles. During the course of this study we found that the PMB/PEB blends remain homogeneous for many hours in the metastable region. Whether or not the RPA can be applied to nonevolving, metastable, single-phase polymer blends is an open question that we address in this paper.

Theoretical Model

We begin with the standard Flory−Huggins expression for the Gibbs energy density change of mixing, ΔG, for a binary mixture of two polymers labeled 1 and 2,[27−29]

$$\frac{\Delta G}{kT} = \left[\frac{\phi_1 \ln \phi_1}{v_1 N_1} + \frac{\phi_2 \ln \phi_2}{v_2 N_2}\right] + \frac{\chi}{v_0}\phi_1\phi_2 \qquad (2)$$

where k is the Boltzmann constant, ϕ_i is the volume fraction of component i in the mixture, N_i is the number of monomers per chain of component i, v_i is the volume of each monomer of component i, χ is the Flory−Huggins interaction parameter, and v_0 is an arbitrary reference volume which we set equal to 100 Å^3. The first term in the right-hand side (RHS) of eq 2 is equal to $-\Delta S/k$ where ΔS is the entropy change of mixing. The second term in the RHS of eq 2 is equal to $\Delta H/kT$ where ΔH is the enthalpy change of mixing.

In most experimental papers, χ is reported as a function of either $1/T$ or P.[1,3,4,6,7,10,11,19−23] We therefore

consider the generalized Gibbs−Helmholtz relation for the dependence of $\Delta G/kT$ on $1/T$ and P, at constant composition[24,30,31]

$$\mathrm{d}\left(\frac{\Delta G}{kT}\right) = \frac{\Delta H}{k}\,\mathrm{d}\left(\frac{1}{T}\right) + \frac{\Delta V}{kT}\,\mathrm{d}P \tag{3}$$

Any equation for the temperature and pressure dependence of ΔG such as eq 2 must comply with eq 3. It is also clear from eqs 2 and 3 that if ΔG (or, equivalently, χ) depends on P, then ΔV must be finite. On the other hand, the original Flory−Huggins equation (eq 2) was derived under the assumption that $\Delta V = 0$ and $\Delta H = \Delta U$, where ΔU is the internal energy change of mixing. The χ parameter for a blend in perfect compliance with the Flory−Huggins theory would be independent of P.

We propose a simple extension of the Flory−Huggins theory that accounts for finite ΔV. This extension is similar to that used to account for the pressure dependence of thermodynamics of regular solutions.[31] We assume that ΔV is given by the expression

$$\Delta V = v\phi_1(1-\phi_1)/v_0 \tag{4}$$

Our expression for ΔV is analogous to the Flory−Huggins expression for ΔU:

$$\frac{\Delta U}{kT} = u\phi_1(1-\phi_1)/v_0 \tag{5}$$

In eqs 4 and 5, v and u for a pair of polymers are assumed to be independent of blend composition and component molecular mass. At a given T and P, ΔH ($=\Delta U + P\Delta V$) is given by

$$\frac{\Delta H}{kT} = \left(u + \frac{Pv}{kT}\right)\phi_1(1-\phi_1)/v_0 \tag{6}$$

It is clear that eq 1 can be used to determine the T and P dependence of ΔG if we redefine χ as

$$\chi(T,P) = u(T) + \frac{v(T)}{kT}P \tag{7}$$

We assume that functions u and v are dependent only on temperature. Equation 7 thus predicts that χ at a given temperature is a linear function of pressure. This prediction is consistent with a large fraction of the experimental data on polymer blends.[1,4,6,7,10,11] In the limit $P \to 0$, $\chi \equiv u$.

The boundary between the single-phase and two-phase regions of the phase diagram of binary blends that obey the Flory−Huggins theory—the binodal curve—is obtained by solving the following equations:

$$\ln\left(\frac{\phi_1^{\mathrm{I}}}{\phi_1^{\mathrm{II}}}\right) + (\phi_1^{\mathrm{II}} - \phi_1^{\mathrm{I}})(1 - N_1v_1/N_2v_2) + \frac{\chi(T,P)N_1v_1}{v_0} \times ((1-\phi_1^{\mathrm{I}})^2 - (1-\phi_1^{\mathrm{II}})^2) = 0 \tag{8a}$$

$$\ln\left(\frac{1-\phi_1^{\mathrm{I}}}{1-\phi_1^{\mathrm{II}}}\right) + (\phi_1^{\mathrm{I}} - \phi_1^{\mathrm{II}})(1 - N_2v_2/N_1v_1) + \frac{\chi(T,P)N_2v_2}{v_0}((\phi_1^{\mathrm{I}})^2 - (\phi_1^{\mathrm{II}})^2) = 0 \tag{8b}$$

where ϕ_1^{I} and ϕ_1^{II} are the volume fractions of component 1 in the coexisting phases at the temperature and pressure of interest. Equations 8a and 8b are the Clausius−Clayperon equations for binary polymer blends. The spinodal curve (the limit of instability of the one-phase system), for Flory−Huggins blends, is given by

$$\frac{\partial^2(\Delta G/kT)}{\partial\phi_1^{\,2}} = \left(\frac{1}{N_1v_1\phi_1} + \frac{1}{N_2v_2\phi_2}\right) - 2\,\frac{\chi(T,P)}{v_0} = 0 \tag{9}$$

The above results, when combined with the two-step derivation of the RPA equation given by Higgins and Benoit,[32] demonstrate the consistency of the RPA at any temperature and pressure. In the first step, Higgins and Benoit show that the scattering intensity for a blend of two noninteracting polymers labeled 1 and 2 (i.e., $\chi = 0$) is given by

$$I(q) = \left(\frac{b_1}{v_1} - \frac{b_2}{v_2}\right)^2\left(\frac{1}{S_{11}^0(q)} + \frac{1}{S_{22}^0(q)}\right)^{-1} \tag{10}$$

where the partial structure factors S_{ii}^0 are given by

$$S_{ii}^0(q) = N_iv_i\phi_iP_i(q) \quad (i = 1, 2) \tag{11}$$

$P_i(q)$ is the Debye function of the i chains,

$$P_i(q) = \frac{2}{x^2}(\mathrm{e}^{-x} + x - 1) \tag{12}$$

where $x = q^2R_{\mathrm{g},i}^2$, $R_{\mathrm{g},i} = N_il_i^2/6$, and l_i is the statistical segment length of polymer i. It is obvious that eqs 10−12 apply at any temperature and pressure. The only parameters in these equations that depend on T and P are l_i and v_i;[33] both parameters are only weakly dependent on T and P. The T and P dependence of the monomer volumes, v_i, is obtained from PVT measurements on the pure homopolymers. For the polymers used in this study (PMB and PEB), the PVT results can be summarized by eq 13

$$v_i = v_{i,\mathrm{ref}}\exp\left[\alpha_i(T - T_{i,\mathrm{ref}}) + (\beta_i - \gamma_iT)(P - P_{i,\mathrm{ref}})\right] \tag{13}$$

where $v_{i,\mathrm{ref}}$ is the monomer volume at a reference temperature and pressure ($T_{i,\mathrm{ref}}$ and $P_{i,\mathrm{ref}}$, respectively) and constants α_i, β_i, and γ_i are experimentally determined parameters.[34] The T and P dependence of l_i is obtained from SANS experiments, as described in the next section.

In binary polymer mixtures, it has been shown the scattered intensity due to density fluctuations is negligible when compared to the scattered intensity due to concentration fluctuations.[32,35−37] In this case, the scattering intensity in the forward direction is given by

$$I(q\to 0) = I_0 = \left(\frac{b_1}{v_1} - \frac{b_2}{v_2}\right)^2\left(\frac{\partial^2(\Delta G/kT)}{\partial\phi_1^{\,2}}\right)^{-1} \tag{14}$$

In the second step of the derivation, Higgins and Benoit correct eq 10 to comply with eq 14. Combining eqs 2, 10, and 14 yields the familiar RPA result,

$$I(q) = \left(\frac{b_1}{v_1} - \frac{b_2}{v_2}\right)^2\left(\frac{1}{S_{11}^0(q)} + \frac{1}{S_{22}^0(q)} - \frac{2\chi}{v_0}\right)^{-1} \tag{15}$$

Note that in our approach χ is redefined to include ΔV

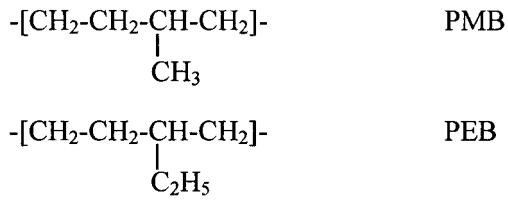

Figure 2. Chemical structures of the monomer units for the polymers used in this study.

Table 1. Characteristics of Polymers

polymer	density (g/cm^3)	av no. of D atoms per 6 C atoms	mol mass (g/mol)	polydispersity index
*d*PMB	0.9300	7.33	1.8×10^5	1.07
*h*PEB1	0.8629	0	4.8×10^4	1.07
*h*PEB2	0.8628	0	2.2×10^5	1.08

contributions according to eq 7. Since eqs 2, 7, 10, and 14 are valid at any T and P, it follows that eq 15 is valid at any T and P.

Equations 2, 7, 10, and 15 are the main results of this section. These equations may be considered as a simple extension of the mean-field theory of polymer blends that is consistent with the generalized Gibbs−Helmholtz equation. The weak T and P dependence of ΔS (which is due to the T and P dependence of the monomer volumes, v_i) makes our framework slightly inconsistent with the generalized Gibbs−Helmholtz equation. The inconsistency is not of practical significance if the variation of χ with pressure is significantly larger than the isothermal compressibility, i.e., $|\partial \ln(\chi)/\partial P| \gg |\partial \ln(v_i)/\partial P|$. Blends wherein the variation of χ with pressure is similar in magnitude to the isothermal compressibility are in prefect agreement with the original Flory−Huggins theory.[11,35]

A powerful feature of the RPA is that it can address the thermodynamics of a diverse array of polymer systems such as block copolymer melts and complex multicomponent mixtures that are outside the realm of the Flory−Huggins theory. Pressure-dependent SANS data from such systems will be discussed in future publications.

Experimental Section

Hydrogeneous and partially deuterated polymethylbutylene (PMB) and polyethylbutylene (PEB) homopolymers were synthesized and characterized using methods described in refs 38 and 39. The chemical formulas of the (majority) repeat units in these polymers are given in Figure 2. These chemical moieties also serve as definitions of monomer units for purposes of theoretical computations. The characteristics of the polymers used in this study are given in Table 1. Hydrogenous polymers are referred to with a prefix *h* while the deuterium-labeled polymer is referred to with a prefix *d*. Binary blends of PMB and PEB were made by dissolving the components in cyclohexane and drying to a constant weight in a vacuum oven at 70 °C. The compositions of the blends studied here are given in Table 2.

The *PVT* properties of PMB and PEB homopolymers were measured by Krishnamoorti.[34] We use his results to estimate the temperature and the pressure dependence of the monomer volume of each of the species using eq 13. The parameters to be used in eq 13 for the polymers used in this study are given in Table 3.

SANS experiments were conducted on the NG3 beamline at the National Institute of Standards and Technology in Gaithersburg, MD. The SANS data reported here were obtained in three separate runs, each lasting 3−4 days. The samples were held in a thermostated steel pressure chamber between two sapphire windows separated by a 1.5 mm Teflon O-ring. (After assembly of the pressure cell, the O-ring is squeezed to a thickness of approximately 1 mm.[40]) The samples were made by placing the O-ring on top of one of the sapphire windows and adding the required amount of polymer (ca. 0.16 g) in the region enclosed by the O-ring. The polymer, O-ring, and window were then placed in a vacuum oven at 80 °C for ca. 8 h. Heating caused the polymer sample to flow and occupy the space provided by the O-ring. The assembly was then carefully placed in the pressure cell and capped with the second sapphire window. The pressure cell was connected to a reservoir of silicone oil, which served as the pressurizing fluid. A computer-driven piston assembly was used to control the sample pressure. A more detailed description of the pressure cell is given in ref 9.

Table 2. Composition of Samples Studied

sample	components A	components B	ϕ_A[a]
B1	*d*PMB	*h*PEB1	0.414
B2	*d*PMB	*h*PEB1	0.203
B3	*d*PMB	*h*PEB2	0.161
B4	*d*PMB	*h*PEB2	0.099

[a] Volume fraction of component A is computed at 30 °C and atmospheric pressure, based on weight fraction of the components and measured densities of the components.[33] The magnitudes of ΔV, and the mismatch in the thermal expansion coefficients and the isothermal compressibilities of the components, are too small to have a significant effect on ϕ_A.

The SANS data from blends B1 and B2 were obtained using the following configuration: neutron wavelength, $\lambda = 6.0$ Å, wavelength spread, $\Delta\lambda/\lambda = 0.15$, sample-to-detector distance = 9 m, sample aperture = 0.635 cm, source-to-sample distance = 8.57 m, and source size = 5.0 cm. The configuration used for blends B3 and B4 was slightly different from the configuration for the blends B1 and B2: the sample-to-detector distance = 11 m, and the source-to-sample distance = 10.12 m; all other settings were the same. A kinetic experiment was performed on blend B3 using the following configuration: neutron wavelength, $\lambda = 14.0$ Å, wavelength spread, $\Delta\lambda/\lambda = 0.15$, sample-to-detector distance = 13.18 m, sample aperture = 0.635 cm, source-to-sample distance = 14.77 m, and source size = 5.0 cm. For the static measurements, the time for data acquisition was 5−20 min, depending on the scattered intensity. Data acquisition was started 5−10 min after the cell temperature and pressure had equilibrated. The scattering data were collected using a 128 × 128 pixel two-dimensional detector, corrected for background scattering, empty cell scattering, and detector sensitivity. All of the scattering profiles were azimuthally symmetric. We thus report the azimuthally averaged scattering intensity as a function of q [$q = 4\pi \sin(\theta/2)/\lambda$, θ is the scattering angle]. The raw data from the static measurements were converted to absolute scattering intensity, $I(q)$, using methods and secondary standards described ref 23. The data from the kinetic measurements were not converted to absolute scattering intensity.

Estimates of errors in our measurements are provided in the Appendix.

Experimental Results

Our first experiments on PMB/PEB blends were conducted on blends B1 and B2 where the short PEB chains were used. These blends were studied as a function of increasing temperature from 29 to 103 °C. At each temperature, the pressure was increased from 0.01 to 1 kbar. On the basis of previous studies,[23] we were sure that these blends were in the single-phase region at atmospheric temperature and pressure. We did not anticipate phase separation in these blends and therefore did not investigate the effect of thermal and compression history. Typical data are shown in Figure 3 where we show the pressure dependence of $I(q)$

Table 3. Temperature and Pressure Dependence of Monomer Volume, v_i

component	T_{ref} (K)	P_{ref} (kbar)	v_{ref} (Å^3)	α (K^{-1})	β (kbar^{-1})	γ (K^{-1} kbar^{-1})
PMB	300.15	1.01×10^{-3}	136.2	6.8×10^{-4}	-6.40×10^{-2}	4.03×10^{-4}
PEB	300.15	1.01×10^{-3}	162.0	7.1×10^{-4}	-7.12×10^{-2}	4.22×10^{-4}

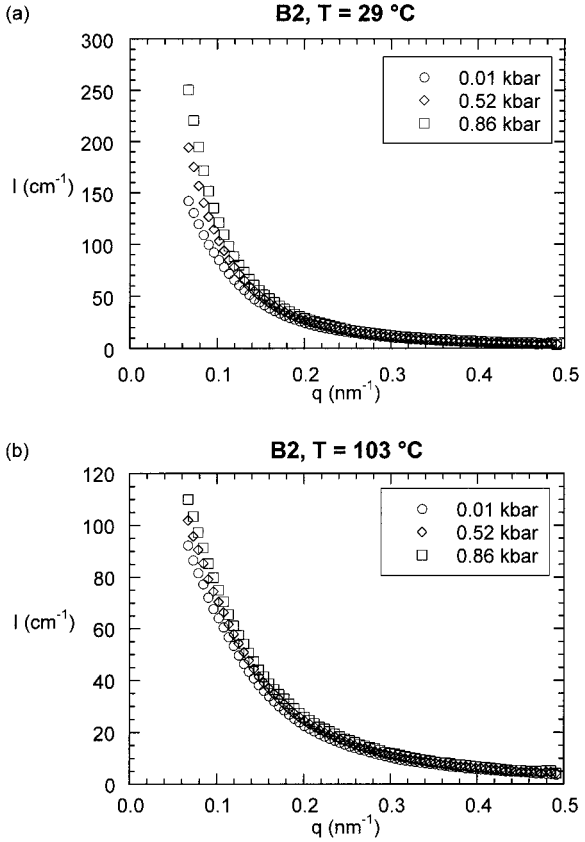

Figure 3. SANS intensity versus the scattering vector (I versus q) from blend B2 at (a) 29 °C and (b) 103 °C, at selected pressures.

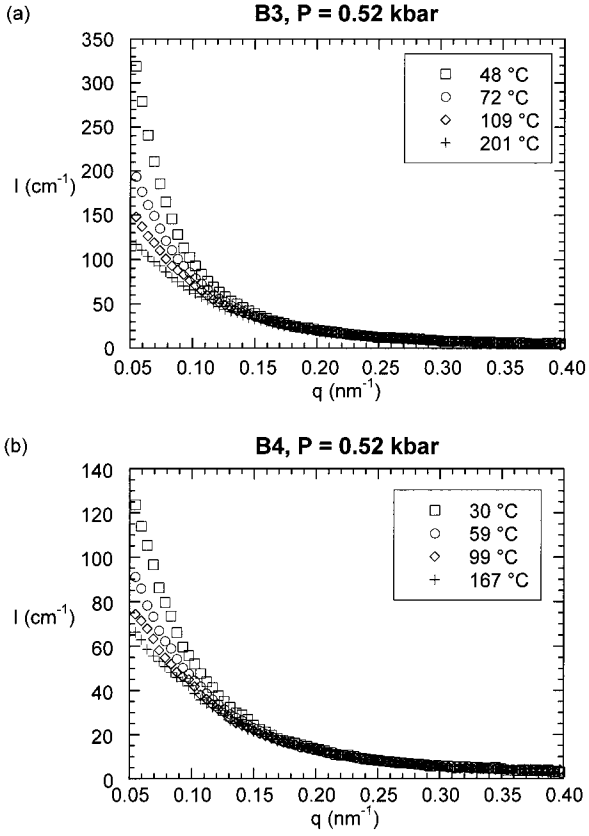

Figure 4. SANS intensity versus the scattering vector (I versus q) at a pressure of 0.52 kbar for (a) blend B3 and (b) blend B4, at selected temperatures.

obtained at 29 °C (Figure 3a) and 103 °C (Figure 3b) from sample B2. It is evident that pressure has a larger effect on $I(q)$ at the low temperature (29 °C) than at the high temperature (103 °C).

The experimental protocol used to study blends B3 and B4 was quite different from that used for blends B1 and B2, because we anticipated that these blends were in the two-phase region at atmospheric temperature and pressure. Note that the long PEB chains were used to make these blends. We therefore studied blends B3 and B4 as a function of thermal history; i.e., they were studied as a function of increasing as well as decreasing temperature. As was the case with blends B1 and B2, at each temperature, the blends were studied as a function of increasing pressure. In Figure 4 we show the temperature dependence of $I(q)$ at $P =$ 0.52 kbar for blends B3 (Figure 4a) and B4 (Figure 4b). Both sets of data were obtained during the cooling run after the sample was heated to 201 °C for blend B3 and 167 °C for blend B4. In Figure 5a, we show the low-q scattering data from blend B3 at $P = 0.52$ kbar (Figure 4a) in the Zimm format: $1/I$ versus q^2. The lines in Figure 5a are least-squares linear fits through the data. Zimm plots of the low-q data from blend B4 at $P = 0.52$ kbar are shown in Figure 5b. We use the Zimm plots to extrapolate the $I(q)$ data and estimate I_0, the scattering intensity as $q \rightarrow 0$.

We obtained I_0 by this procedure for both blends B3 and B4 at each temperature and pressure, during both heating and cooling runs. In Figure 6a we show the temperature dependence of $1/I_0$ of B3 at $P = 0.01$ kbar (which is essentially atmospheric pressure). During the heating run (circles in Figure 6a), the sample was heated from room temperature to 201 °C. A sharp discontinuity in the temperature dependence of I_0 is seen in the heating run at $T = 127$ °C. In contrast, no discontinuity is seen during the cooling run, which was conducted in two segments. First, the sample was cooled from 201 °C after completion of the heating run to 109 °C and studied as a function of decreasing temperature until $T = 42$ °C (triangles). In the second segment, the sample was reheated to 91 °C and studied as a function of decreasing temperature from $T = 78$ to 60 °C (squares).

The sharp discontinuity in the heating data at 127 °C in Figure 6a is an indication that blend B3 had undergone a phase transition. In fact, the values of I_0 obtained below 100 °C, during the heating run, are negative. This is an unambiguous signature of a two-phase system. The true value of I_0 must be positive; the negative values of I_0 indicate the presence of large domains that are outside the instrument resolution (q range). It is perhaps interesting to note that blend B3 was optically transparent when it was loaded into the pressure cell at 23 °C, despite the presence of the large domains. This is undoubtedly due to the weak optical contrast between the domains and the matrix. On the other hand, the neutron contrast between the domains

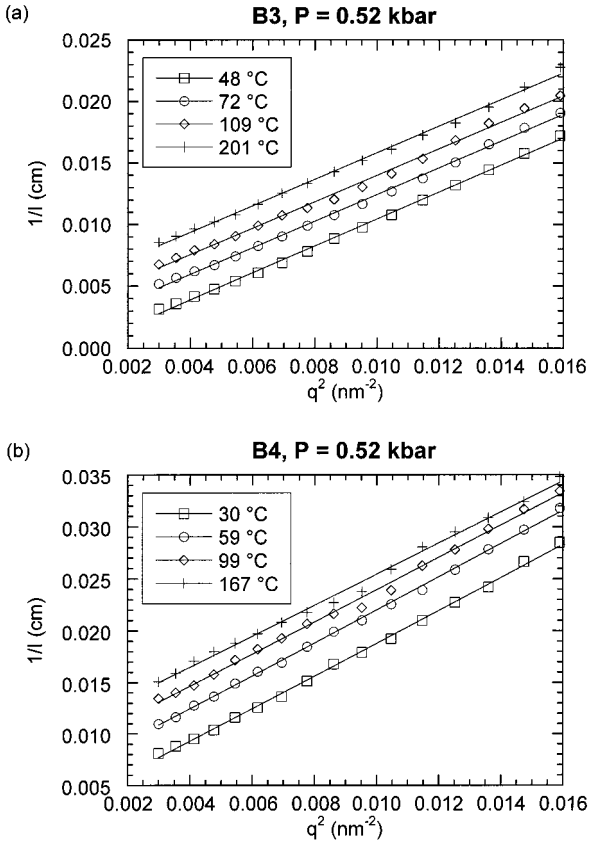

Figure 5. Inverse of the SANS intensity, $1/I$, versus q^2 at various temperatures, for (a) blend B3 and (b) blend B4, at a constant pressure of 0.52 kbar. The solid lines are least-squares linear fits through the data.

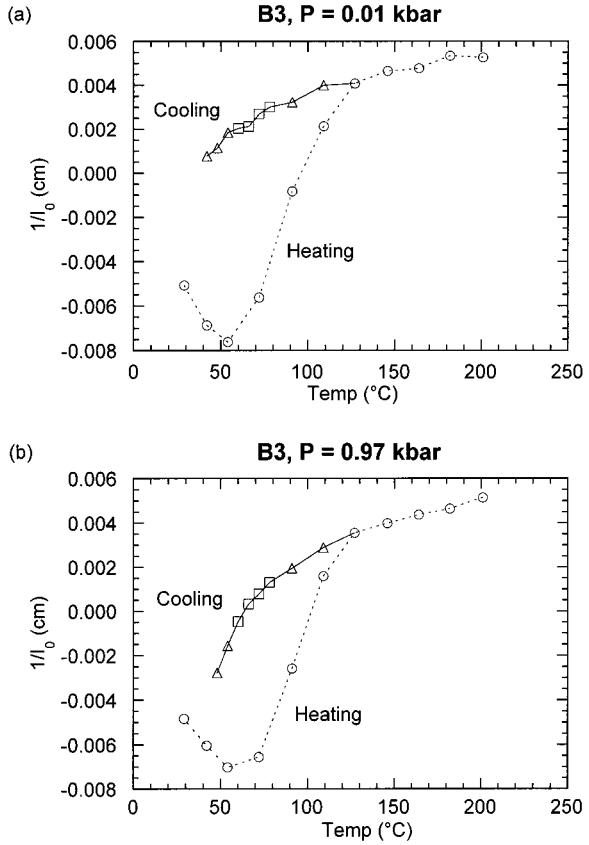

Figure 6. Extrapolated inverse SANS intensity as $q \rightarrow 0$, $1/I_0$ versus temperature T for blend B3 at (a) 0.01 kbar and (b) 0.97 kbar.

and the matrix is considerably larger due to deuteration of the PMB chains. Thus, the two-phase state of blend B3 at room temperature is only evident in a neutron scattering experiment. In Figure 6b we show $1/I_0$ versus T data from sample B3 at the highest pressure ($P =$ 0.97 kbar). The $P = 0.97$ kbar data (Figure 6b) are qualitatively similar to the $P = 0.01$ kbar data (Figure 6a). In both cases we can identify two branches for the $1/I_0$ versus T curves, a heating branch and a cooling branch.

It is tempting to think of the junction point of the heating and cooling branches in Figure 6a,b as the location of the binodal. It undoubtedly indicates the transition from a two-phase state to a single-phase state upon heating. However, caution must be exercised, due to the long chain character of the components, and the resulting potential of observing nonequilibrium effects. Molecular motion in blends B3 and B4 is extremely slow. On the basis of viscoelastic properties,[42,43] we estimate that the longest molecular relaxation times for the PMB and PEB chains in blends B3 and B4 are 10 and 0.6 s, respectively. The kinetics of dissolution of macrophases composed of such sluggish molecules as a function of the blend location in the phase diagram is not known. We may require considerable superheating to dissolve the macrophases on the experimental time scale (order of minutes). From our previous publications, it is evident that increasing pressure on PMB/PEB systems increases χ; i.e., it increases the incompatibility.[11] This indicates that the binodal temperature at $P = 0.97$ kbar should be higher than that at 0.01 kbar. However, we know that the phase separation kinetics in these PMB/PEB blends at low quench depths is very slow.[12] Thus, once the system has been brought into the single-phase region, it remains single phase even after it has been superpressurized (or undercooled) into the two-phase region. We thus conclude that the junction point of the heating and cooling branches at $P = 0.01$ kbar (127 °C, see Figure 6a) is an upper limit for the binodal temperature at $P = 0.01$ kbar. On the other hand, there is no significance to the junction point of the heating and cooling branches at $P = 0.97$ kbar (Figure 6b) due to nonequilibrium effects.

The dependence of $1/I_0$ on T for blend B4 at $P = 0.01$ kbar is shown in Figure 7a while that at $P = 1.00$ kbar is shown in Figure 7b. Here we see no effect of thermal and compression history; the $1/I_0$ versus T data for the heating and cooling runs are within the noise level of the measurements. We are thus not able to obtain any estimate of the location of the binodal in blend B4.

We are now interested in applying the RPA-based analysis to the $I(q)$ data obtained from our samples. Since the RPA-based analysis applies only to single-phase systems, we need to determine the T,P range over which samples B1 through B4 are single phase. This is particularly important for samples B3 and B4, which were designed to be located near the phase boundary. However, hysteresis and slow kinetics prevented us from obtaining information about the binodal curves, except for the conclusion that 127 °C is an upper limit for the binodal temperature of blend B3 at atmospheric pressure. Our only remaining alternative is to locate the phase boundary, using eq 8. However, we have not yet determined $\chi(T,P)$, so we cannot use eq 8. We thus have

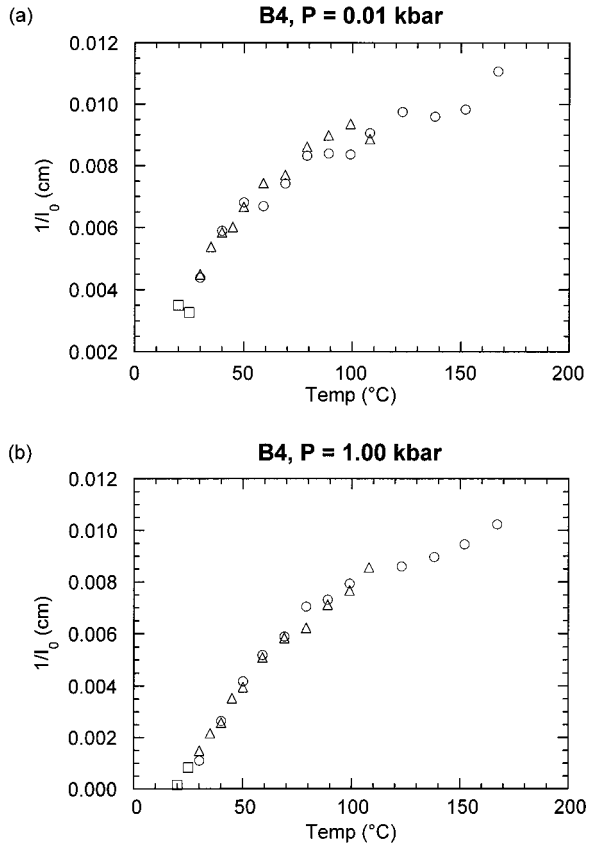

Figure 7. Extrapolated inverse SANS intensity as $q \rightarrow 0$, $1/I_0$ versus temperature T for blend B4 at (a) 0.01 kbar and (b) 1.00 kbar.

a dilemma. We know that we can use the RPA for systems in the single-phase region to obtain $\chi(T,P)$. We also know that we cannot use the RPA for systems inside the spinodal. We are not sure whether the RPA can be applied to the data in the metastable region. Our problem, however, is that without knowing $\chi(T,P)$ we do not know where the boundaries between these regions lie.

Our solution to this dilemma was to simply analyze all of the available data using the RPA-based equations and examine the validity of the analysis after this was done. The procedure used for analyzing the data was identical to that used in our previous publications.[22,23,39] In Figure 8a, we show the pressure dependence of $I(q)$ obtained from sample B1 at 66 °C. The sample is well within the one-phase region of the phase diagram at all pressures. The curves through the data represent least-squares RPA fits (eq 15) with χ and l_i as adjustable parameters. All other parameters are obtained from independent experiments, and a summary of these parameters is given in Table 4. From our previous studies,[39] we know the statistical segments lengths for PMB and PEB chains at atmospheric temperature and pressure ($l_{i,\mathrm{ref}}$). The values of l_i of both PMB and PEB were changed by a constant factor α, relative to $l_{i,\mathrm{ref}}$,

$$l_i(T,P) = \alpha l_{i,\mathrm{ref}} \quad (i = 1, 2) \tag{16}$$

to obtain the best fit. It is appropriate to think of α as an average expansion factor for the two chains.

The theoretical curves in Figure 8a are thus two-parameter fits with χ and α as adjustable parameters. It is evident that there is good agreement between theory and experimental data from sample B1. The

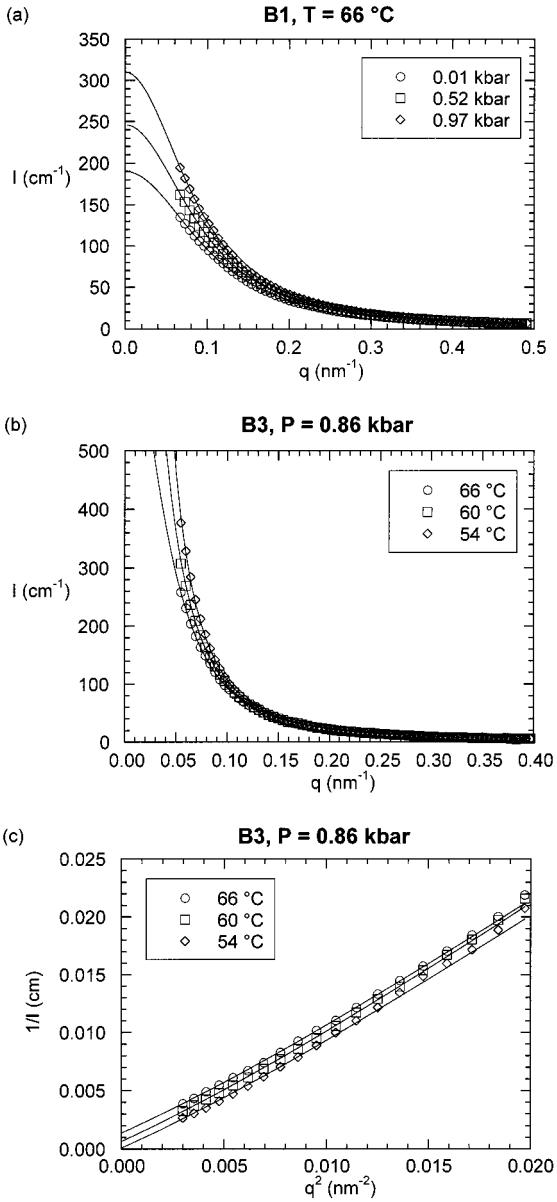

Figure 8. SANS intensity, I, versus q, for (a) blend B1 at various pressures at a constant temperature of 66 °C and (b) blend B3 at selected temperatures with a constant pressure of 0.86 kbar. (c) The data in (b) is shown in the $1/I$ versus q^2 format. The divergence of $I(q)$ at low q is due to the proximity of B3 to the spinodal. Blend B1 is located in the single-phase region, whereas blend B3 is located in the metastable two-phase region. The solid lines through the data in (a), (b), and (c) represent least-squares RPA fits.

Table 4. Parameters Used for RPA Calculations

parameter	*d*PMB	*h*PEB1	*h*PEB2
N_i	2465	525	2630
v_i (Å^3/monomer)	136.2	162.0	162.0
$l_{i,\mathrm{ref}}$ (Å)	8.26	7.93	7.93
b_i (Å)	5.95×10^{-4}	-4.98×10^{-5}	-4.98×10^{-5}

procedure described above for sample B1 was repeated on the data obtained from all four samples. In the case of B3 and B4 we used the data obtained during the cooling runs, after the sample had been heated into the one phase region. In Figure 8b, we show the comparison between theory and experiment for sample B3 at selected temperatures and $P = 0.86$ kbar. On the basis of our previous estimates of χ,[23] we expect B3 to be well inside the two-phase region at these values of T and P.

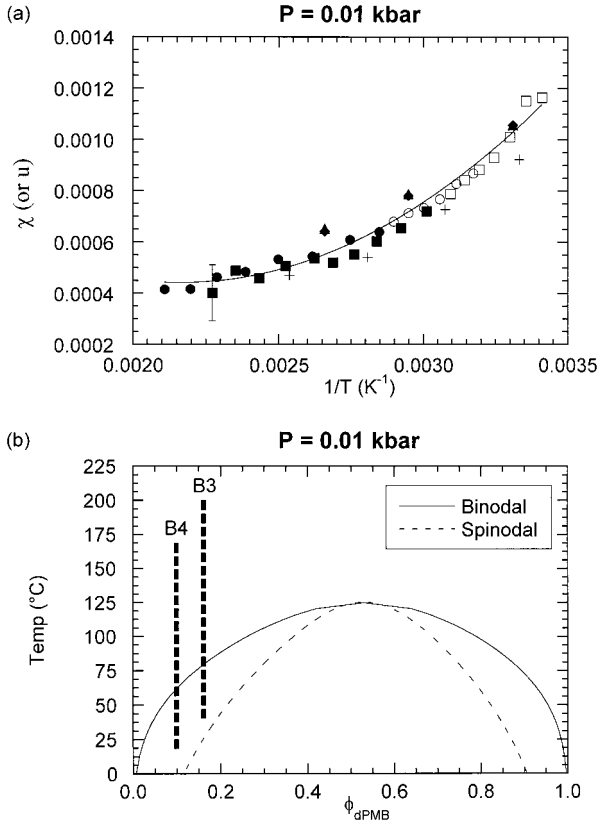

Figure 9. (a) Dependence of χ on $1/T$ at a pressure of 0.01 kbar. Diamonds, B1; triangles, B2; circles, B3; and squares, B4. The filled symbols indicate results from blends in the one-phase region. The unfilled symbols indicate results from blends in the metastable two-phase region. The pluses represent previously published data for a *d*PMB/*h*PEB blend taken at atmospheric pressure.[23] The error bar shows the largest error in χ. The curve is the least-squares quadratic fit through the present data. At $P = 0.01$ kbar, χ is approximately equal to u. (b) Calculated phase diagram for blends B3 and B4 at 0.01 kbar in T versus ϕ_{dPMB} format. The parameters used for the T dependence of χ are $A = 0.002\,53$, $B = -1.929$ K, and $C = 446.01$ K^2. The solid curve is the binodal curve, and the thin dashed curve is the spinodal curve. The thick vertical dashed lines show the range at which χ values were determined for samples B3 and B4.

Despite this, the RPA works rather well; the quality of the fits obtained from B3 at 0.86 kbar (Figure 8b) is similar to that obtained from B1 at 66 °C (Figure 8a). Because of the proximity of blend B3 to the spinodal, the extrapolated intensity as $q \rightarrow 0$ is very large. This is best seen in a Zimm plot where we plot $1/I$ versus q^2 (Figure 8c). At 54 °C, $I(q \rightarrow 0)$ is 10^4 cm^{-1} and the sample is estimated to be 4 °C from the spinodal.

In Figure 9a we show the results of the fitting procedure for all of the samples at $P = 0.01$ kbar in the form of χ versus $1/T$. The pluses shown in Figure 9a represent previously published data[23] for the temperature dependence of χ at atmospheric pressure between *d*PMB and *h*PEB measured on a critical mixture with a relatively low molecular mass *h*PEB. The temperature dependence of χ that we have obtained from samples B1 through B4 is in good agreement with previously published data at atmospheric pressure. Just as we had done in our previous studies on PMB/PEB blends,[10,23] we assumed that χ was a quadratic function of $1/T$

$$\chi = A + B/T + C/T^2 \qquad (17)$$

The solid curve in Figure 9a represents the best least-squares fit through the data, which gives us the parameters A, B, and C. Knowing χ as a function of T enables us to determine the phase diagram for any of the *d*PMB/*h*PEB blends at $P = 0.01$ kbar. We found, as we had expected, that blends B1 and B2 are single-phase in the entire temperature window at 0.01 kbar. In Figure 9b, we thus show the phase diagram for *d*PMB/*h*PEB2 blends (B3 and B4). The vertical dashed lines represent the range of temperatures at which χ values were reported in Figure 9a. Note that a substantial portion of the measurements on samples B3 and B4 were conducted in the metastable region of the phase diagram. The filled symbols in Figure 9a represent the data taken from stable, single-phase systems, while the open symbols represent the data taken from metastable systems. The fact that χ measurements from the metastable region from samples B3 and B4 agree quantitatively with those obtained from B1 and B2 in the single-phase region indicates that the RPA equations provide an accurate description of the concentration fluctuations in metastable polymer blends. To our knowledge, these are the first experimental tests of the applicability of the RPA to metastable systems. The subject of metastable liquids is of considerable current interest.[44] Binary PMB/PEB blends may be model systems for studying metastability, due to the ease with which metastable states can be obtained and the applicability of a mean field theory in this regime.

In Figure 10a we show typical χ versus $1/T$ data obtained at elevated pressures ($P = 0.86$ kbar). The data are qualitatively similar to those obtained at $P = 0.01$ kbar (Figure 9a). We fit the data in Figure 10a using eq 17 to get $\chi(T)$ at $P = 0.86$ kbar and then use eqs 8 and 9 to compute the phase diagram for *d*PMB/*h*PEB2 blends at $P = 0.86$ kbar. The results are shown in Figure 10b. As expected, we find that a significant fraction of *d*PMB/*h*PEB2 data (samples B3 and B4) was obtained from metastable, single-phase samples. It is evident that the χ parameters obtained from stable and metastable single-phase samples are in good agreement at atmospheric (Figure 9a) as well as elevated (Figure 10a) pressures.

We were able to compute the phase diagrams at all of the pressures studied, using the same procedure that was used to produce Figures 9b and 10b. In Figure 11a, we show a temperature−pressure phase diagram for the blend B3. The dashed lines in Figure 11a indicate the locations of the calculated binodal and spinodal curves. To obtain experimental confirmation of the blend B3 phase diagram, we conducted a two-part kinetic experiment, described schematically by the arrows in Figure 11a. The first part is a phase separation experiment, and the second part is a two-step dissolution experiment.

In the phase separation experiment, sample B3 was quenched from the one-phase region to 48 °C at 0.86 kbar (point A in Figure 11a). Point A is located deep in the two-phase region and is, in fact, within the estimated spinodal. Time zero for this part of the experiment is when the sample reached 48 °C and 0.86 kbar. The SANS profiles obtained after the quench showed the classic scattering signatures for spinodal decomposition; the time dependence of the SANS profiles is shown in Figure 11b. A scattering peak developed during the early stages of phase separation. At later times, the peak moved toward the beamstop due to coarsening processes.

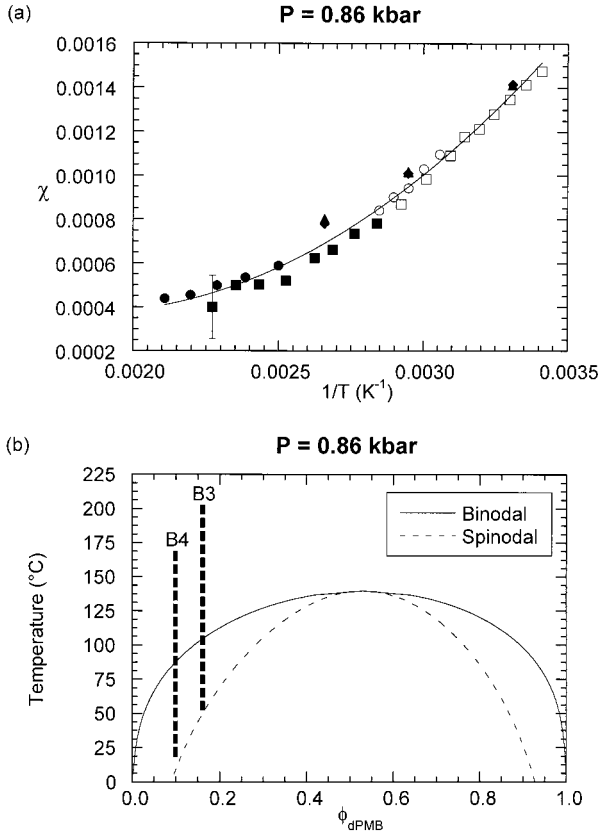

Figure 10. (a) Dependence of χ on $1/T$ at a pressure of 0.86 kbar. Diamonds, B1; triangles, B2; circles, B3; squares, B4. The filled symbols indicate results from blends in the one-phase region. The unfilled symbols indicate results from blends in the metastable two-phase region. The error bar shows the largest error in χ. The curve is the least-squares quadratic fit through the data. (b) The calculated phase diagram for blends B3 and B4 at 0.01 kbar in T versus ϕ_{dPMB} format. The parameters used for the T dependence of χ (eq 15) are $A = 0.001\,85$, $B = -1.628$ K, and $C = 449.01$ K^2. The solid curve is the binodal curve, and the thin dashed curve is the spinodal curve. The thick vertical dashed lines show the range at which χ values were determined for samples B3 and B4.

After keeping the sample at point A for about 9 h, the dissolution experiment was begun by heating the sample at constant pressure to 91 °C (point B in Figure 11a). Note that point B is quite close to the binodal curve but still within the two-phase region. Time zero for the dissolution experiment is when the sample reached 91 °C at 0.86 kbar. We kept the sample at point B for 1 h, and the SANS profiles obtained during the A → B step of the dissolution experiment are shown in Figure 11c. The SANS intensity did decrease slightly during the early stages of the A → B step but then stopped changing as shown in Figure 11c. After 1 h, the SANS intensity was orders of magnitude larger than that obtained from homogeneous blends, indicating that we were not able to homogenize the blend at point B. This result is consistent with the phase diagram in Figure 11a, which indicates that point B is located inside the two-phase region. The second step of the dissolution experiment (started at $t = 89$ min) was to depressurize and heat the blend to 0.01 kbar and 109 °C, which is above the predicted binodal curve (point C in Figure 11c). The equilibration time for the pressure cell after initiating a temperature change is considerable, and in Figure 11c, we show the SANS profiles obtained after the sample had equilibrated at point C which was about 1 h after the B → C step was initiated. The B → C step

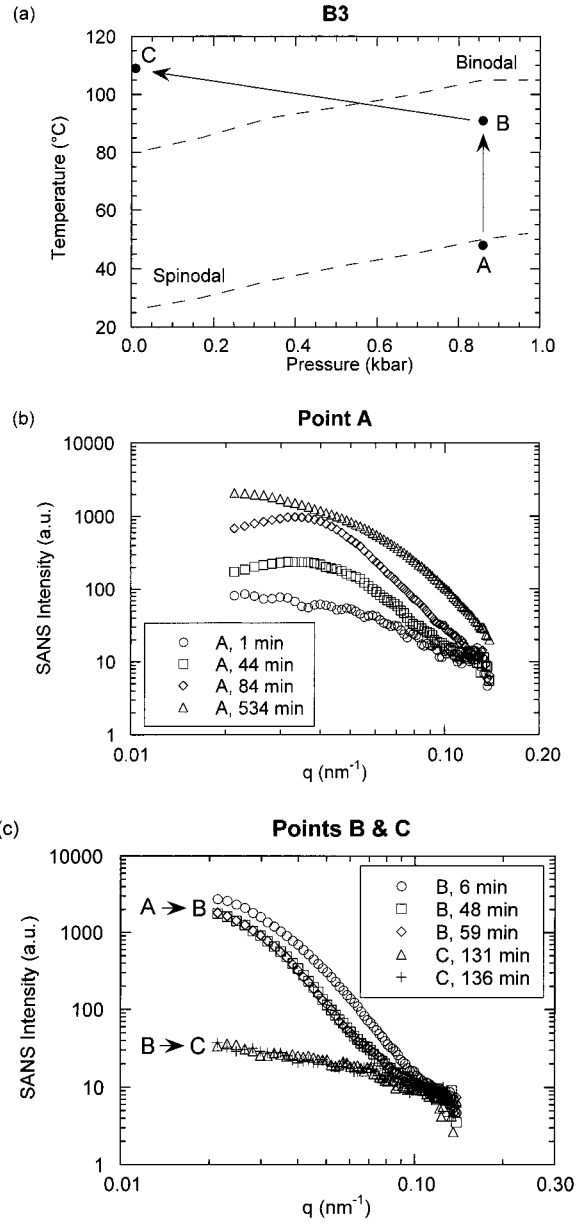

Figure 11. (a) Calculated phase diagram for blend B3 in T versus P format. Points A (48 °C, 0.86 kbar), B (91 °C, 0.86 kbar), and C (109 °C, 0.01 kbar) indicate the points at which kinetic experiments were performed. Blend B3 was quenched from the single-phase region to A, then from A to B, and finally from B to C. (b) The time dependence of the relative SANS intensity versus scattering vector q during phase separation at point A. (c) The time dependence of the SANS intensity following the A → B and B → C steps. The B → C step results in dissolution of the two-phase structure, consistent with the phase diagram in (a).

resulted in a 2 orders of magnitude decrease in the SANS intensity, and we obtained data characteristic of single-phase samples (see Figure 11c).

It is evident that the kinetic data obtained during the A → B → C quench confirm our phase diagram calculations that were based entirely on static SANS data. Thus, 109 °C is our best experimental estimate of the binodal temperature of blend B3 at atmospheric pressure. Note that this is an upper bound because finite superheating is required to dissolve the two-phase structure in a finite amount of time. Our previous estimate of the binodal temperature of blend B3 at atmospheric pressure, based on 5 min experiments

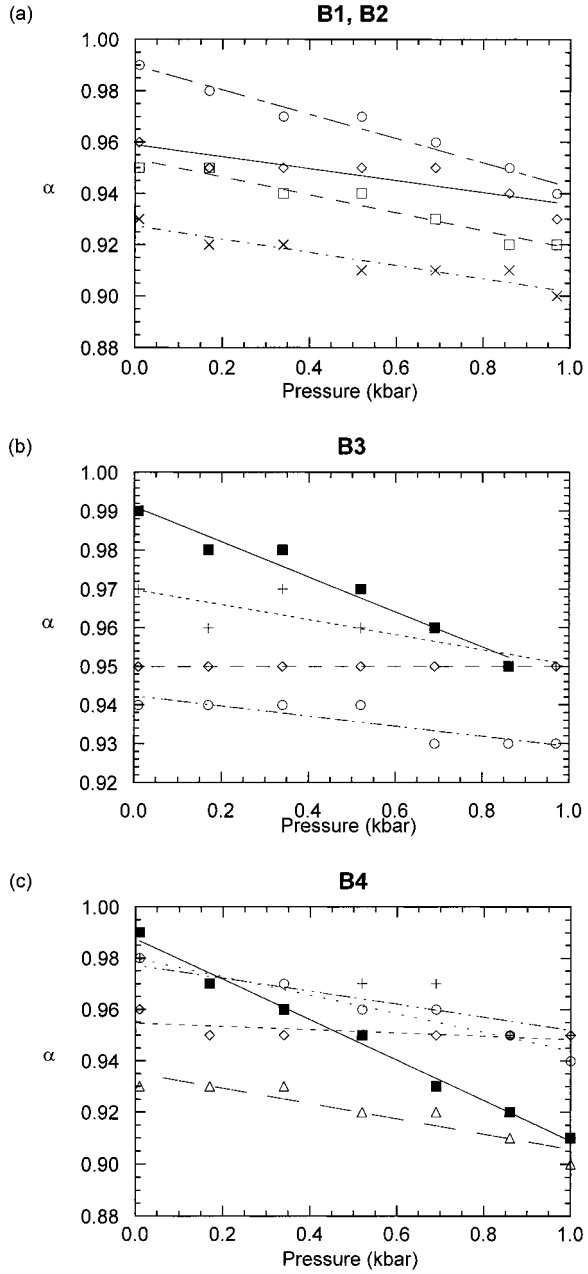

Figure 12. Expansion factor, α, versus pressure for (a) blends B1 and B2. The circles and diamonds are for blend B1 at 29 and 103 °C, respectively. The squares and crosses are for blend B2 at 29 and 103 °C, respectively. (b) Blend B3. Filled squares, $T = 54$ °C; pluses, $T = 78$ °C; diamonds, $T = 146$ °C; circles, $T = 201$ °C. (c) Blend B4. Filled squares, $T = 20$ °C; circles, $T = 30$ °C; pluses, $T = 35$ °C; diamonds, $T = 79$ °C; triangles, $T = 167$ °C. The lines are least-squares linear fits to the data.

(Figure 6a), was 127 °C. The new estimate of 109 °C, which is based on a much longer experiment (the experiment took 12 h to complete), is closer to the calculated binodal temperature of 80 °C. By conducting longer experiments and taking finer steps, one could presumably verify the location of the binodal with greater accuracy. However, finite beam time prevented us from doing so.

Thus far we have focused on χ, which is related to the scattering intensity as $q \rightarrow 0$. We now discuss results obtained for α, which is related to the scattered intensity at finite q, and reflects the average expansion of the chains in the blend. In Figure 12a we show the pressure dependence of α at selected temperatures for samples

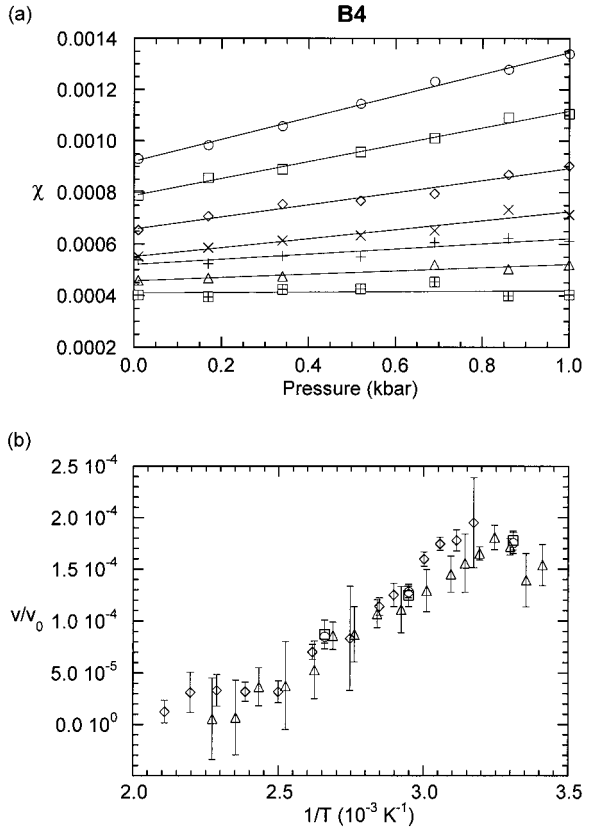

Figure 13. (a) Flory−Huggins χ parameter versus pressure for blend B4 at selected temperatures. Circles, $T = 35$ °C; squares, $T = 50$ °C; diamonds, $T = 69$ °C; crosses, $T = 89$ °C; pluses, $T = 108$ °C; triangles, $T = 138$ °C; hatched squares, $T = 167$ °C. The solid lines are least-squares fits through the data. The slope equals v/kT and the intercept equals u. (b) The dependence of v/v_0 ($v_0 = 100$ Å^3) on $1/T$ for all blends. Circles, B1; squares, B2; diamonds, B3; triangles, B4.

B1 and B2. We find that α decreases with pressure, corresponding to a coil shrinkage of about 2% per kbar, regardless of temperature. In Figure 12b we show the pressure dependence of α at selected temperatures for sample B3. At temperatures between 201 and 60 °C we see coil shrinkage of about 2% per kbar. The magnitude of the shrinkage is in agreement with that obtained from samples B1 and B2. At temperatures less than 60 °C, however, a steeper dependence of α on P is obtained (filled symbols in Figure 12b). We speculate that this is due to a departure of the concentration fluctuations in the blend from the RPA prediction. Note that at these temperatures the deviations are relatively subtle, with a reduction in R_g ranging between 4 and 6% from the expected value and a χ that is indistinguishable from stable single-phase systems (Figure 9a). Similar deviations in the dependence of α on P are obtained in blend B4. However, the deviations become evident at 30 °C, as shown in Figure 12c.

In the theoretical section it was shown that u, the parameter that gives the magnitude of ΔU, is equal to χ at $P = 0$ (which is very well approximated by atmospheric pressure). Thus, the temperature dependence of u for PMB/PEB blends is simply given by Figure 9a. It was also shown in the theoretical section that ΔV is related to the pressure dependence of χ. For PMB/PEB blends, the χ parameter was independent of sample composition (see Figures 9a and 10a). It is therefore sufficient to show χ versus P for one of the blends. In Figure 13a we show χ versus P for blend B4

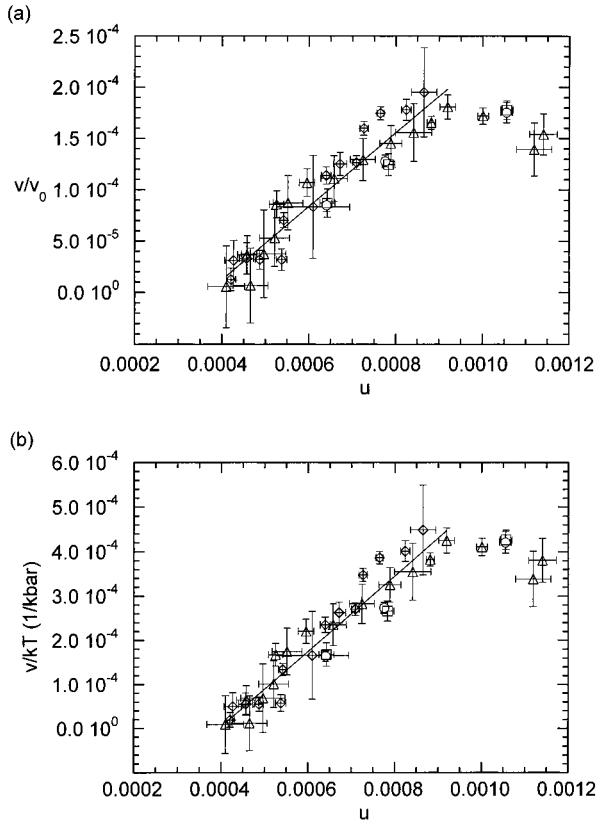

Figure 14. Relationship between the volume change of mixing (ordinate) and internal energy change of mixing (abscissa): (a) v/v_0 versus u; (b) v/kT versus u. Circles, B1; squares, B2; diamonds, B3; triangles, B4. The solid lines are the least-squares linear fits through the $u \leq 0.001$ data.

at selected temperatures. A linear pressure dependence is seen at all temperatures in agreement with eq 7. The lines through the data in Figure 13a represent least-squares fits, and the slope is set equal to v/kT. The intercept is set equal to u. The temperature dependence of v/v_0 is shown in Figure 13b. Since we expect the blends to approach ideal mixing at higher temperatures, it is likely that v/v_0 (i.e., ΔV) will be a decreasing function of T. Equation 7 thus predicts that the slope of χ versus P will decrease with temperature. The data in Figure 13a,b are in agreement with this expectation.

In our previous paper[11] we had noted that ΔU and ΔV in PMB/PEB blends were interrelated [notice the similarity in Figure 9a for $u(T)$ and Figure 13b for $v(T)$]. In particular, we noticed that the volume change parameter v/v_0 was approximately a linear function of u. In Figure 14a we plot v/v_0 versus u obtained from all of the blends. It is evident in Figure 14a that the v versus u data can be approximated by a straight line ($u < 0.001$). However, we realized that other functional forms for the v dependence of u may be applicable. In Figure 14b, we replot the data in the format of v/kT versus u. The reason for making this plot will be made clear shortly. We find that this plot can also be approximated by a straight line. There is little difference in the goodness of the fit in Figure 14a,b. The problem is that the accessible temperature window (20−200 °C) is, in fact, a very limited window, when one looks on the $1/T$ scale (T is absolute temperature). Thus, on the basis of the PMB/PEB data we can assert the existence of a relationship between u and v, although the exact functional form is still in doubt.

Let us examine the consequences of a linear relationship between v and u. Let us assume that u is of the form $u = A + B/T + C/T^2$ as it is for our blends. If we assume that v is a linear function of u, then eq 7 indicates that χ at high pressures would have a cubic dependence on $1/T$, i.e., $\chi = A + B'/T + C'/T^2 + D'/T^3$. The temperature dependence of the high-pressure data (e.g., Figure 10a) from PMB/PEB blend is entirely consistent with a quadratic dependence, as is the case at atmospheric pressure. Thus, the implication of a linear dependence between v and u implies a complexity that is not evident in any of the data that we have obtained. On the other hand, it is straightforward to see that this difficulty vanishes if we assume that v/kT is a linear function of u.

$$v/kT = D + Eu \tag{18}$$

In this case, the same functional form applies to the χ versus $1/T$ data at atmospheric and elevated pressures. This is consistent with our observations. It is thus more reasonable to conclude that for the PMB/PEB system v/kT is a linear function of u as depicted in Figure 14b. For PMB/PEB blends, we conclude that $D = -0.000\,337$ (1/kbar) and $E = 0.853$ (1/kbar). The linear relationship between v/kT and u is restricted to small values of u ($u < 0.001$). When $u \geq 0.001$, we see a substantial departure from linear behavior in both parts a and b of Figure 14. The linear fits in Figure 14a,b are thus restricted to data wherein $u < 0.001$.

A linear relationship between u and v/kT is not unreasonable. According to the Flory−Huggins theory,[28,29] the magnitude of u is a measure of the difference between the energy of interactions between unlike monomers (ϵ_{12}) and the average of the energy of interaction between like monomers [$(\epsilon_{11} + \epsilon_{22})/2$]. This difference leads to a net repulsion between unlike chains that results in phase separation when u is sufficiently large. It is natural for the chains to move apart from each other due to these repulsive interactions, i.e., a positive ΔV (or v). One can thus view v as a response to u, and in the case of weakly interacting systems, one might expect a linear response. Most linear responses hold over a limited range of parameters. Our experiments indicate that the linear response of v to u is limited to $u < 0.001$ and $v/kT < 0.0004$ (1/kbar). Further work is need to establish the underpinnings of the temperature and pressure dependence of u and v.

Concluding Remarks

We have developed a simple framework for studying the temperature and pressure dependence of the thermodynamics of polymer blends. We have shown that:

(1) The RPA is equally valid at atmospheric and elevated pressure, provided the χ parameter is redefined to include contributions due to ΔU and ΔV.

(2) The measured pressure dependence of χ provides a direct measure of ΔV, in accordance with the generalized Gibbs−Helmholtz relationship (eq 3).

(3) Our framework leads to a consistent set of equations for analyzing the results of type I (eqs 2, 7, and 15) and type II (eq 8) experiments.

(4) The Clausius−Clayperon equation for binary blends (eq 8) differs substantially from the one-component Clausius−Clayperon equation (eq 1).

We have thus answered the questions that were presented in the Introduction.

The proposed reason for the pressure (P) dependence of the χ parameter is, in many respects, analogous to the classical interpretation of the temperature ($1/T$) dependence of χ.[45,46] In most polymer blends, the measured χ parameter is a linear function of $1/T$ at fixed P ($\chi = A + B/T$), wherein the slope B is interpreted as the enthalpic contribution (ΔH) to χ, and the intercept A is interpreted as the entropic contribution (ΔS) to χ. However, the $1/T \rightarrow 0$ limit is impossible to reach due to polymer degradation, and the uncertainty of the extrapolated value of χ at $1/T = 0$ is extremely large. Consequently, there is considerable debate about the significance of the parameter A. In most polymer blends, the measured χ parameter is a linear function of P at fixed T ($\chi = D + EP$). A linear χ versus P plot is a natural consequence of the present work, wherein the slope E is interpreted as the volumetric (ΔV) contribution to χ, and the intercept D is interpreted as the internal energy (ΔU) contribution to χ. In contrast, with the available temperature ($1/T$) window, the $P \rightarrow 0$ limit is conveniently obtained experimentally: atmospheric pressure is a very good approximation of zero pressure (see Figure 13a). There is thus less room for debate about the significance of the measured intercept of the χ versus P plots. In our framework, we assume that ΔU and ΔV depend on temperature only and are independent of pressure. The only effect of pressure is to amplify the importance of the $P\Delta V$ contribution to the Gibbs energy of mixing, ΔG. In other words, phase separation in polymer blends such as PMB/PEB is induced by the application of pressure because the volume of the phase-separated state is smaller than that of the homogeneous state, and the Gibbs energy is lowered through mechanical work ($P\Delta V$). Similarly, the magnitude of the concentration fluctuations in single-phase PMB/PEB blends increases upon the application of pressure because the volume of the system decreases with increasing magnitude of the concentration fluctuations.

Our interpretation differs substantially from a recent proposal by Rabeony et al.[6] The pressure-dependent SANS data that they have obtained from a number of different polyolefin blends are consistent with the notion of a pressure-dependent solubility parameter. The implication of these experiments is that the pressure dependence of χ provides a direct measure of the pressure dependence of ΔU. We note, however, that simply introducing a pressure-dependent ΔU into the conventional Flory−Huggins theory makes the theory inconsistent with the generalized Gibbs−Helmholtz relationship. In polymer blends with specific interactions, it is very likely that ΔU will depend on pressure. In such cases where ΔU changes significantly with pressure, a new framework that is consistent with the Gibbs−Helmholtz relationship will be needed for analyzing the data. Our work suggests that such effects may be manifested by a nonlinear dependence of χ on P (e.g., ref 3).

We have used the proposed framework to analyze SANS data obtained from a series of off-critical PMB/PEB blends. We estimate parameters related to the internal energy change of mixing (u) and the volume change of mixing (v) from the measured temperature and pressure dependence of the χ parameter. We find that a linear relationship between v/kT and u holds for small values of u and v, suggesting that the increase in volume obtained upon mixing is a linear response to the repulsive interactions between monomers.

We also explored the metastable nature of blends B3 and B4 as a function of temperature and pressure. When we start with either of the blends that has been aged in the two-phase region for a long time (e.g., 1 week), we find that they must be heated to a temperature well above the estimated binodal to obtain a single-phase system. After homogenization, we found that we could undercool and superpressurize our blends to temperatures and pressures well within the binodal without causing any observable phase separation on our experimental time scale (5 min to several hours). For example, for blend B3 at 0.86 kbar, we could undercool the blend to 50 °C below the binodal. The χ parameters and the statistical segment lengths obtained by fitting the data from undercooled blends in the metastable region are very similar to those determined from stable, single-phase blends well removed from a phase boundary. This indicates that the concentration fluctuations in the metastable region of the phase diagram have the same character as those in stable, single-phase blends that have been extensively analyzed by the RPA-based theory.

Acknowledgment. We thank Sanat Kumar for educational discussions and Chenchy Lin, Ramanan Krishnamoorti, and S. V. Jonnalagadda for their contributions during the initial stages of this project. Financial support from the National Science Foundation (CTS-9805852, DMR-9457950) and the Dreyfus Foundation to Polytechnic University is gratefully acknowledged. The SANS instrument at NIST is supported by the National Science Foundation (DMR-9423101).[47]

Appendix. Estimates of Errors

The sources of errors in determining thermodynamic properties of polymer blends from SANS measurements are discussed in ref 22. The following error estimates are based on the accuracy of the characterization methods: N_i, 5%; v_i, 0.1%; ϕ_i, 0.1%; b_i, 3%. Typical errors in the estimate of χ and l_i are 18% and 4%, respectively (error bars for χ decrease with proximity of the blend to the spinodal). Far away from the spinodal the error in χ is as much as 36%. The reason for the increased uncertainty in χ is discussed in ref 40. The uncertainties in the temperatures and pressures reported in this paper are 0.2 °C and 0.01 kbar, respectively.

References and Notes

(1) Janssen, S.; Schwahn, D.; Mortensen, K.; Springer, T. *Macromolecules* **1993**, *26*, 5587.
(2) Janssen, S.; Schwahn, D.; Springer, T.; Mortensen, K. *Macromolecules* **1995**, *28*, 2555.
(3) Schwahn, D.; Frielinghaus, H.; Mortensen, K.; Almdal, K. *Phys. Rev. Lett.* **1996**, *77*, 3153.
(4) Hajduk, D. A.; Urayama, P.; Gruner, S. M.; Erramilli, S.; Register, R. A.; Brister, K.; Fetters, L. J. *Macromolecules* **1995**, *28*, 7148.
(5) Hajduk, D. A.; Gruner, S. M.; Erramilli, S.; Register, R. A.; Fetters, L. J. *Macromolecules* **1996**, *29*, 1473.
(6) Rabeony, M.; Lohse, D. J.; Garner, R. T.; Han, S. J.; Graessley, W. W.; Migler, K. B. *Macromolecules* **1998**, *31*, 6511.
(7) Hammouda, B.; Bauer, B. *Macromolecules* **1995**, *28*, 4505.
(8) Hammouda, B.; Benmouna, M. *J. Polym. Sci., Polym. Phys. Ed.* **1995**, *33*, 2359.
(9) Hammouda, B.; Balsara, N. P.; Lefebvre, A. A. *Macromolecules* **1997**, *30*, 5572.
(10) Balsara, N. P.; Lefebvre, A. A.; Lee, J. H.; Lin, C. C.; Hammouda, B. *AIChE J.* **1998**, *44*, 2515.
(11) Lefebvre, A. A.; Lee, J. H.; Balsara, N. P.; Hammouda, B.; Krishnamoorti, R.; Kumar, S. *Macromolecules* **1999**, *32*, 5460.

(12) Lefebvre, A. A.; Lee, J. H.; Jeon, H. S.; Balsara, N. P.; Hammouda, B. *J. Chem. Phys.* **1999**, *111*, 6082.
(13) Beiner, M.; Fytas, G.; Meier, G.; Kumar, S. K. *Phys. Rev. Lett.* **1998**, *81*, 594.
(14) Pollard, M.; Russell, T. P.; Ruzette, A. V.; Mayes, A. M.; Gallot, Y. *Macromolecules* **1998**, *31*, 6493.
(15) Migler, K. B.; Han, C. C. *Macromolecules* **1998**, *31*, 360.
(16) de Gennes, P. G. *Scaling Concepts in Polymer Physics*; Cornell University Press: Ithaca, NY, 1979.
(17) Leibler, L. *Macromolecules* **1980**, *13*, 1602.
(18) Hammouda, B. *Adv. Polym. Sci.* **1993**, *106*, 87.
(19) Jeon, H. S.; Lee, J. H.; Balsara, N. P. *Macromolecules* **1998**, *31*, 3328.
(20) Jeon, H. S.; Lee, J. H.; Balsara, N. P.; Newstein, M. C. *Macromolecules* **1998**, *31*, 3340.
(21) (a) Herkt-Maetzky, C.; Schelten, J. *Phys. Rev. Lett.* **1983**, *51*, 896. (b) Hadziioannou, G.; Stein, R. S. *Macromolecules* **1984**, *17*, 567. (c) Han, C. C.; et al. *Polymer* **1988**, *29*, 2002. (d) Bates, F. S.; et al. *J. Chem. Phys.* **1988**, *89*, 535. (e) Graessley, W. W.; et al. *Macromolecules* **1995**, *28*, 1260.
(22) Balsara, N. P.; Fetters, L. J.; Hadjichristidis, N.; Lohse, D. J.; Han, C. C.; Graessley, W. W.; Krishnamoorti, R. *Macromolecules* **1992**, *25*, 6137.
(23) Lin, C. C.; Jonnalagadda, S. V.; Balsara, N. P.; Han, C. C.; Krishnamoorti, R. *Macromolecules* **1996**, *29*, 661.
(24) Van Ness, H. C.; Abbott, M. M. *Classical Thermodynamics of Non Electrolyte Solutions*; McGraw-Hill: New York, 1982.
(25) Bidkar, U.; Sanchez, I. C. *Macromolecules* **1995**, *28*, 4505.
(26) Tang, H.; Freed, K. F. *Macromolecules* **1991**, *24*, 958.
(27) Staverman, A. J.; Van Saten, J. H. *Recl. Trav. Chim.* **1941**, *60*, 76.
(28) Huggins, M. L. *J. Phys. Chem.* **1942**, *46*, 151.
(29) Flory, P. J. *J. Chem. Phys.* **1942**, *10*, 51.
(30) Prigogine, I.; Bellemans, A.; Mahot, V. *The Molecular Theory of Solutions*; North-Holland: Amsterdam, 1957; Chapter 8.
(31) Prausnitz, J. M.; Lichenthaler, R. N.; de Avezedo, E. G. *Molecular Thermodynamics of Fluid-Phase Equilibria*; Prentice Hall: Englewood Cliffs, NJ, 1986.
(32) Higgins, J. S.; Benoit, H. C. *Polymers and Neutron Scattering*; Oxford Univeristy Press: New York, 1994.
(33) The volume changes estimated from our experiments are sufficiently small so that ϕ is essentially independent of pressure. Similarly, contributions due to isothermal compressibility of the components are negligible.
(34) Krishnamoorti, R. Ph.D. Thesis, Princeton University, Princeton, NJ, 1994.
(35) Kumar, S. *Macromolecules* **2000**, *33*, 5285.
(36) It is conventional in some groups to subtract the volume fraction weighted scattering from the pure components from the measured scattering from blends.[37] As long as density fluctuations in a given blend are a linear combination of the density fluctuations in the pure components, the SANS intensity profiles will not contain contributions due to density fluctuations.
(37) Balsara, N. P.; Lohse, D. J.; Graessley, W. W.; Krishnamoorti, R. *J. Chem. Phys.* **1994**, *100*, 3905.
(38) Rachapudy, H.; Smith, G. G.; Raju, V. R.; Graessley, W. W. *J. Polym. Sci., Polym. Phys. Ed.* **1979**, *17*, 1211.
(39) Balsara, N. P.; Jonnalagadda, S. V.; Lin, C. C.; Han, C. C.; Krishnamoorti, R. *J. Chem. Phys.* **1993**, *99*, 10011.
(40) After the experiments presented in this paper were completed, it was established that the sample thickness, d, when the pressure cell is loaded with the correct amount of polymer is 1.16 ± 0.01 mm. During the early days when these experiments were carried out, it was believed that $d = 1.0$ mm. A micrometer for measuring the separation between the windows was not available at that time. It is known, however, that transmission coefficient, t, in polyolefin blends is a sensitive function of d. For synthetic polymer blends, t is dominated by the incoherent scattering from H atoms.[41] $t = \exp(-n\sigma_H d)$ where n is the H atom concentration per unit volume, σ_H is the effective incoherent scattering cross section of H atoms, and d is the sample thickness. During our experiments, we became suspicious of the advertised d value due to small, otherwise inexplicable differences in the measured values of t. Using a sample thickness of 1.16 mm for B3, we obtain $\sigma_H = 1.05 \times 10^{-22}$ cm^2, which is in agreement with literature values.[34] Using this value and the measured transmission coefficients of the other samples, we obtained d values of 1.23, 1.24, and 1.05 mm for samples B1, B2, and B4, respectively. The d values obtained correlated well with the amount of sample that was loaded into the pressure cell, and we used these values in our calculations. Note that when we loaded the pressure cell, we thought that d was 1 mm. It was our determination that the separation between the windows was substantially greater than 1 mm that prompted the NIST scientists to obtain the appropriate micrometer. This uncertainty will thus not be an issue in future experiments. The error bars in our estimate of χ have been expanded to account for a 10% uncertainty in sample thickness. This uncertainty does not affect any of the major conclusions of this work.
(41) Maconnachie, A. *Polymer* **1984**, *25*, 1068.
(42) Gotro, J. T.; Graessley, W. W. *Macromolecules* **1984**, *17*, 2767.
(43) Lin, C. C.; Jeon, H. S.; Balsara, N. P.; Hammouda, B. *J. Chem. Phys.* **1995**, *103*, 1957.
(44) Debenedetti, P. G. *Metastable Liquids Concepts and Principles*; Princeton University Press: Princeton, NJ, 1996.
(45) Flory, P. J. *Principles of Polymer Chemistry*; Cornell University Press: Ithaca, NY, 1953.
(46) Balsara, N. P. In *Physical Properties of Polymers Handbook*; AIP Press: Woodbury, NY, 1996; Chapter 19, p 257.
(47) Identification of equipment and materials does not imply recommendation by the National Institute of Standards and Technology.

MA000462X